



**Universiteit  
Leiden**  
The Netherlands

## **Water Line Strengths Toward High-Mass Star Forming Regions: Predictions for Herschel/HIFI**

Doty, S.D.; Tak, F.F.S. van der; Dishoeck, E.F. van; Boonman, A.M.S.

### **Citation**

Doty, S. D., Tak, F. F. S. van der, Dishoeck, E. F. van, & Boonman, A. M. S. (2005). Water Line Strengths Toward High-Mass Star Forming Regions: Predictions for Herschel/HIFI. Retrieved from <https://hdl.handle.net/1887/8277>

Version: Not Applicable (or Unknown)

License: [Leiden University Non-exclusive license](#)

Downloaded from: <https://hdl.handle.net/1887/8277>

**Note:** To cite this publication please use the final published version (if applicable).

## WATER LINE STRENGTHS TOWARD HIGH-MASS STAR FORMING REGIONS: PREDICTIONS FOR HERSCHEL/HIFI.

S. D. Doty<sup>1</sup>, F. F. S. van der Tak<sup>2</sup>, E. F. van Dishoeck<sup>3</sup>, and A. M. S. Boonman<sup>3</sup>,  
<sup>1</sup>Department of Physics and Astronomy, Denison University, Granville, OH 43023, USA (doty@denison.edu),  
<sup>2</sup>Max-Planck-Institut für Radioastronomie, Auf dem Hügel 69, 53121 Bonn, Germany, <sup>3</sup>Sterrewacht Leiden, PO Box 9513, 2300 RA Leiden, The Netherlands

**Introduction:** The structure and evolution of high-mass star-forming regions is generally murkier than their low-mass counterparts, due to their short lifetimes, relative infrequency of formation, and relatively larger distances from the Earth. Recent data from ISO and SWAS have provided significant data on molecular lines in these regions that are difficult to observe from the ground. Of particular interest is water. This is due not only to its important role in thermal balance of the gas, and its status as the main repository of oxygen not locked up in CO, but also due to its strong correlation with temperature: at low temperatures (< 100K) it is mostly frozen onto grain mantles, while at higher temperatures (>100-300K) it is mostly in the gas-phase. Herschel (under development and due for launch in 2007) is the fourth cornerstone mission in the Horizon 2000 ESA science program. It is a 3.5m class satellite telescope, with high angular resolution (11''.3 at 157  $\mu$ m), and high signal to noise. The HIFI spectrometer on Herschel is expected to yield very high ( $R = \lambda/\Delta\lambda \sim 10^6 - 10^7$ ) spectral resolution in the range 0.48-1.25 THz and 1.41-1.91 THz. This range covers 14 transitions of ortho-H<sub>2</sub>O, when considering the first 25 energy levels ranging from 34K to  $\sim 1090$ K above the ground state. As such, it will be uniquely poised to probe the chemical and thermal structure of massive protostellar envelopes from their presumably hot-core interiors to their cold, envelope-like exteriors. Toward this end, we present models of a range of high-mass protostellar cores, and provide predictions for the water emission / absorption relevant to HIFI / Herschel from these regions.

**Model:** The models presented here are similar to those presented in a multi-transition study of H<sub>2</sub>O from a set of high-mass YSOs [1]. The physical structure, dust temperatures, and gas temperature distribution for each source is taken from self-consistent modeling [2,3,4], and the resulting temperature and density profiles for a number of the sources is given in Fig. 1. The H<sub>2</sub>O abundance is taken to be a rough step-function at 100K, in agreement with recent infall / evolutionary modeling [5]. The water distribution for each source are given in Table 1. The radiative transfer for the gas is calculated self-consistently using the ALI method [4], and has been tested against various benchmarks [6,7]. Given the lack of detailed

source geometry, no systematic velocity gradient is included, but a turbulent doppler  $b$  of 2 km/s is adopted. The collisional rates are taken from the literature [8,9]. The cloud is assumed to be initially cold and to have collapsed in less than the ortho-para H<sub>2</sub> conversion time of  $\sim 10^6$  yrs, yielding an ortho:para ratio of o-H<sub>2</sub>:p-H<sub>2</sub> = 1:0. We have also considered the effects of an infinite temperature (3:1) ratio and an in-between case (1:1).

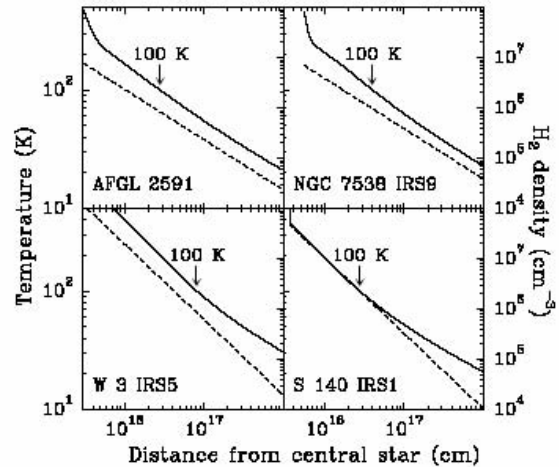


Figure 1. The distribution of temperature (solid line) and density (dashed line) as a function of position for four of the sources considered.

Source	Ice evaporation	Freeze-out	Cold gas-phase H <sub>2</sub> O	$N(\text{H}_2\text{O}_{\text{ice}})^b$	$T_{\text{ex}}(\text{C}_2\text{H}_2)^c$ (K)
AFGL 2591	YES, $T \sim 90-110$ K	YES, $T \leq 90-110$ K	$x(\text{H}_2\text{O}) \sim 0-10^{-3}$	1.7(18)	900
NGC 7538 IRS1	YES	YES, $T \leq 90-110$ K	$x(\text{H}_2\text{O}) \leq 10^{-4}$	3.1(18)	500
W 3 IRS5	YES, $T \sim 90-110$ K	YES, $T \leq 90-110$ K	$x(\text{H}_2\text{O}) \leq 10^{-3}$	5.1(18)	500
S 140 IRS1	?	YES, $T \leq 100$ K	$x(\text{H}_2\text{O}) \sim 0$	2.0(18)	390
MonR2 IRS3	YES, $T \sim 90-110$ K	?	?	1.9(18)	310
NGC 7538 IRS9	NO	YES, $T \leq 100$ K	$x(\text{H}_2\text{O}) \sim 0$	7.0(18)	300

<sup>a</sup>(b) means  $a \times 10^b$ .

<sup>b</sup> The sources are ordered by a decreasing temperature of the warm gas (Lahuis & van Dishoeck 2000).

<sup>c</sup> H<sub>2</sub>O ice column densities from Gibb & Whitet (2002). H<sub>2</sub>O ice column density for AFGL 2591 from Smith et al. (1989) and for NGC 7538 IRS1 from Gerakines et al. (1999).

<sup>d</sup> C<sub>2</sub>H<sub>2</sub> excitation temperature from Lahuis & van Dishoeck (2000) and Boonman et al. (2003), which is a good tracer of the warm gas. For MonR2 IRS3 and S 140 IRS1 the <sup>13</sup>CO temperatures from Giannakopoulou et al. (1997) and Mitchell et al. (1990) respectively, are listed.

Table 1. The distribution of water in the sources considered, including the existence of ice evaporation at >100K, freeze-out at <100K, and abundance of cold gas-phase water. These distributions are adopted from best-fit multi-transition modeling of H<sub>2</sub>O toward these sources [1].

### Results:

*General:* We find that a wide number of transitions are expected to be in emission. In particular, the average peak line temperatures are expected to be 1-10 K ( $1 \times 10^{-14} - 1 \times 10^{-12}$  ergs  $s^{-1} cm^{-2}$ ). For GL2591 and the physical-chemical model described above, all lines are expected to be in emission, with the higher-lying lines generally being stronger than the lower-lying lines. For example, in GL2591 the strongest lines are predicted to be those at 1.87 THz ( $5_{32} - 5_{23}$ ). This is primarily due to the fact that the higher lying lines more directly probe the warmer gas, which also has the highest density of water. The situation is somewhat different in S140 and W3IRS5. Here the strongest emission lines are somewhat lower energies. This is due to the fact that S140 and W3IRS5 have somewhat lower temperatures, and a steeper density profile (which leads to somewhat higher densities at intermediate positions and temperatures). The strongest lines in these sources are expected to be the 1.16 THz ( $3_{21} - 3_{12}$ ) and 1.72 THz ( $3_{03} - 2_{12}$ ) transitions.

*Scenarios considered:* The water distribution scenarios considered are shown in Fig. 2. Here we plot the assumed water abundance as a function of position in the source, where the “jump” is at approximately 100K to simulate ice evaporation. While these forms are parametric, they have been confirmed by detailed infall / evolutionary modeling [5]. The line strengths are somewhat independent of adopted scenario, so long as the scenario leads to an approximate “best-fit” in the multi-transition modeling [1]. For example, for GL2591, scenarios (8) and (4) corresponding to different levels of cold gas-phase water below  $x = 10^{-8}$  are nearly indistinguishable. The resulting HIFI / Herschel predictions are nearly equivalent, showing that HIFI / Herschel should be insensitive to cold water for  $x(H_2O) < 10^{-8}$ . On the other hand, S140 can be potentially fit by scenarios 3, 5, and 6. While 3 and 5 (variations in the desorption temperature between 90 and 110K) are virtually indistinguishable, there is a significant difference with scenario 6 where ice only accounts for  $x = 10^{-6}$  of the water and the rest is formed in the gas-phase. In this case, the  $2_{12} - 1_{01}$  (1.67 THz) and  $6_{43} - 7_{16}$  (1.57 THz) transitions become 5 times weaker in scenario 6, and the  $5_{32} - 4_{41}$  (0.62 THz) transition goes from weak emission to absorption. Thus, the  $5_{32} - 4_{41}$  transition may be a measure of gas-phase vs. ice-evaporation water production. The same results are generally true for NGC 7538: IRS9 as one transitions between the two multi-wavelength best-fit models (4) and (6).

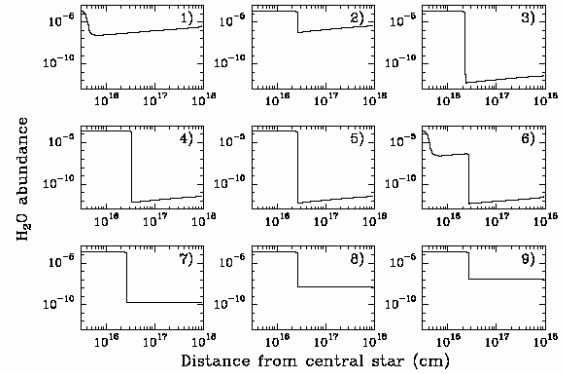


Figure 2. The water abundance distribution as a function of position in the source for various scenarios numbered 1-9. The “jump” corresponds to evaporation of a water ice mantle at  $T \sim 100K$ .

*Absorption.* The lines predicted to be potentially in absorption are the 0.62 THz ( $5_{32} - 4_{41}$ ), 1.57 THz ( $6_{43} - 7_{16}$ ) and 1.88 THz ( $6_{34} - 7_{07}$ ) transitions. The absorption lines are not expected to be strong, especially in comparison to the emission lines. As discussed previously, however, they are somewhat sensitive to the amount of water at “intermediate” (near 100K) temperatures relative to the amount at high (near 200-400K) temperatures. Thus these absorption lines may be able to provide confirmation as to the origin of the gas-phase water.

### References:

- [1] Boonman A. M. S. et al. (2003) *A&A*, 406, 937-955.
- [2] van der Tak F. F. S. et al. (2000) *ApJ*, 537, 283-303.
- [3] Egan M. P., Leung C. M., and Spagna G. F. (1988) *CoPhComm*, 48, 271-292.
- [4] Doty S. D. and Neufeld D. A. (1997) *ApJ*, 489, 122-142.
- [5] Doty S. D., van Dishoeck E. F., and Tan J. C. this volume.
- [6] van Zadelhoff G. J. et al. (2002) *A&A*, 395, 373-384.
- [7] van der Tak F. F. S. et al. (2005) In: *Proceedings of the dusty and molecular universe: a prelude to Herschel and ALMA*, Paris, France, p. 431 – 432.
- [8] Phillips T. R., Maluendes S., and Green S. (1996) *ApJS*, 107, 467-474.
- [9] Green S., Maluendes S., and McLean A. D. (1993), *ApJS*, 85, 181-185.